

R&T 4124072

ANNUAL SUMMARY REPORT

for the period

1 November 1989 through 31 October 1990

for

Office of Naval Research
Contract N00014-89-J-1042

THE DEMONSTRATION OF THE FEASIBILITY OF THE
TUNING AND STIMULATION OF NUCLEAR RADIATION

DTIC
ELECTR
SEP 06 1990
S B D

Short Title: GAMMA-RAY LASER

Principal Investigator: Carl B. Collins

The University of Texas at Dallas
Center for Quantum Electronics
P.O. Box 830688
Richardson, TX 75083-0688

Reproduction in whole, or in part, is permitted for any purpose of the United States Government.

*This document has been approved for public release and sale; its distribution is unlimited.

009

REPORT DOCUMENTATION PAGE		READ INSTRUCTIONS BEFORE COMPLETING FORM
1. REPORT NUMBER XXUV90	2. GOVT ACCESSION NO.	3. RECIPIENT'S CATALOG NUMBER
4. TITLE (and Subtitle) Demonstration of the Feasibility of the Tuning and Stimulation of Nuclear Radiation		5. TYPE OF REPORT & PERIOD COVERED Annual Technical Report 11/1/89 - 10/31/90
		6. PERFORMING ORG. REPORT NUMBER
7. AUTHOR(s) Carl. B. Collins		8. CONTRACT OR GRANT NUMBER(s) N00014-89-J-1042
9. PERFORMING ORGANIZATION NAME AND ADDRESS University of Texas at Dallas P.O. Box 830688 Richardson, TX 75083-0688		10. PROGRAM ELEMENT, PROJECT, TASK AREA & WORK UNIT NUMBERS
11. CONTROLLING OFFICE NAME AND ADDRESS Office of Naval Research Physics Division Arlington, VA 22217		12. REPORT DATE September 1, 1990
		13. NUMBER OF PAGES 34
14. MONITORING AGENCY NAME & ADDRESS (if different from Controlling Office)		15. SECURITY CLASS. (of this report) Unclassified
		15a. DECLASSIFICATION/DOWNGRADING SCHEDULE
16. DISTRIBUTION STATEMENT (of this Report) Approved for public release; distribution unlimited.		
17. DISTRIBUTION STATEMENT (of the abstract entered in Block 20, if different from Report)		
18. SUPPLEMENTARY NOTES		
19. KEY WORDS (Continue on reverse side if necessary and identify by block number) Extreme Ultraviolet Tunable XUV Gamma-Ray Laser		
20. ABSTRACT (Continue on reverse side if necessary and identify by block number) This project concerns the demonstration of the feasibility of the tuning and perhaps even stimulation of nuclear radiation. Theory has indicated that anti-Stokes Raman upconversion of intense but conventional long wavelength sources of radiation produced by scattering from isomeric states of nuclear excitation could lead to significant sources of tunable (continued on next page)		

20. Abstract (continued)

γ -radiation characterized by the natural Mössbauer widths of the lines. This would result in lines with sub-Angstrom wavelengths and widths of a few MHz. Whether or not these processes can reach threshold depends upon the resolution of basic issues lying in an interdisciplinary region between quantum electronics and nuclear physics that have not been previously addressed. It was the purpose of this work to study these issues experimentally.

The overall problem being addressed is a broad one that naturally divides into three lines: 1) Coupling pump power into a nucleus, 2) Extracting nuclear excitation with a radiation field, and 3) Insuring material survival. Such a perspective is beyond the scope of a single project and only the second line has been addressed by the work supported by this grant.

During the current reporting period progress was realized in three areas concerned with the extraction of nuclear excitation with a radiation field. The first continued last year's breakthrough work demonstrating that spin-waves propagating in a host medium could affect nuclear properties. Our most recent focus has been upon the characterization of the spin wave processes to define the opportunities more closely. The second line demonstrated capabilities for tagging photons so that wavetrains with more favorable spectroscopic properties could be selected for use. The third continued the development of advanced instrumentation for the implementation of tagged photon studies at high data collection rates, not previously accessible.

TABLE OF CONTENTS

INTRODUCTION	1
RECENT ACCOMPLISHMENTS	3
REFERENCES	25
APPENDIX I - Reprints of publications appearing during this reporting period	26

INTRODUCTION

The overall objective of our work is to demonstrate the feasibility of a gamma-ray "laser." At gamma-ray wavelengths even the weakest coherent source would be of revolutionary importance, as it would enable the exploitation of the wave properties of gamma radiation. Pursuit of that goal was begun with ONR sponsorship of a contract preceding the current grant. That first phase of research into this broad question of the feasibility of a gamma-ray laser was concerned with problem definition. Evaluations of a number of options finally identified the nuclear analog of the ruby laser as the most likely vehicle for the realization of a gamma-ray laser.¹ The problems were identified as being threefold:

- 1) Coupling pump power into the nucleus,
- 2) Extracting nuclear excitation with the radiation field, and
- 3) Insuring material survival.

Because of the difficulties in developing support for such a breadth of effort in a single activity, the problem was divided roughly along these lines.

The challenge of coupling an intense pulse of some type of pump radiation into the nuclei of a material was spun-off to SDIO. Benefiting from access to large nuclear simulators such as DNA/Aurora at the Harry Diamond Laboratories and to the most intense linacs such as the superconducting injector to the storage ring at Darmstadt the pump mechanism was demonstrated.

A first breakthrough² showed that the energy stored in a long-lived nuclear isomer, $^{180}\text{Ta}^m$ could be dumped into fluorescence with an intense pulse of x-rays by "optically pumping" it through a giant resonance with an integrated cross section approaching $10^{-21} \text{ cm}^2 \text{ eV}$. Such a value is about 1000 times more favorably large than what had been measured for any previous nuclear fluorescence. It represented the discovery of a new class of excitation resonances associated with some collective motion of the nucleus, as yet uncharacterized by theory. This year, in a second breakthrough³ it was shown experimentally that this giant pumping resonance lay at a favorably low excitation energy of 2.8 MeV. *We now know how to pump large amounts of excitation into nuclear systems* and the thrust along the first line of

investigation is turning to the problems of nuclear systematics. The best material to pump must be identified.

Once the nuclei have been pumped (or dumped) the second line of problems becomes of paramount importance. Instead of ending as nuclear fluorescence or as internal conversion, the nuclear excitation must be coupled to the radiation field for controlled extraction. For quite some time we have proposed⁴ the use of resonant, longer wavelength radiation to mix the properties of the nuclear state being pumped by the primary process with properties of another state radiating more freely. In this way the lifetime of the state accumulating the population can be suddenly switched to a shorter value. Very recently Steve Harris has proposed the brilliant concept⁵ of gain without inversion which can be readily adapted to the nuclear environment. Critical to either approach is the ability to affect nuclear populations and to prepare initial quantum states while maintaining natural lifetimes under Mössbauer conditions.

Most laboratory sources of gamma radiation emit at levels of intensity corresponding to single photon conditions and Mössbauer experiments are rarely conducted at such great intensities that the detection of two photons would be probable in the transit time spent between source and absorber. Under those conditions, the perception of gamma rays as streams of particles is instinctive. Nevertheless, as elements of electromagnetic radiation they must also be considered as carrier waves of high frequency and analogs of the multiphoton processes which are routine at the molecular level must be possible at the nuclear scale. For years we had maintained that the key to the excitation of significant levels of multiphoton phenomena lay in the use of small oscillating fields to manipulate the greater ferromagnetic and ferroelectric fields in which the nuclei were immersed. Unfortunately, such materials are almost always magnetostrictive or piezoelectric and the concern had lingered that all coherent phenomena would be overwhelmed and degraded by periodic Doppler shifts produced by vibrations excited by such mechanical efforts. Recently we completed the breakthrough experiment⁶ in which we dressed nuclear states with photons from the periodic oscillation of magnetization transported by spin

waves through a medium unable to propagate vibrations. Large effects were found to confirm our models.

Along the third line of concern to the gamma-ray laser, efforts have been concentrated upon the development of thin film diamond. Diamond has the highest Debye temperature and greatest thermal conductivity of any material. With such a low atomic number there is little absorption of x-rays by the electrons and what is stopped does little damage because the waste heat is readily conducted away. Diamond is the ideal medium into which to insert the nuclei to be pumped with single crystal Be following as a close second. Both will support the Mössbauer effect over as wide a range of aggressive pump conditions as is possible.

In the past few years we have developed a unique means for depositing thin film diamond using a laser plasma source of C^+ ions which are quenched onto a substrate. This seems an ideal environment in which to dope active nuclei, once it becomes known which are the best candidates. The properties and techniques for preparing our laser plasma diamond appear in the literature^{7,8} and further development and even commercialization for other purposes is being supported by an Austin, Texas company, Research Applications, Inc.

RECENT ACCOMPLISHMENTS

Unhappily, breakthroughs do not come every year, and we did not have one during this reporting period. Rather we are presenting our sustained progress toward the extracting of nuclear excitation with a radiation field. This line of investigation, itself divides into three efforts

- a) Studies of spin waves,
- b) Exploitation of tagged photons,
- c) Development of instrumentation.

The first represents a continuation along the path identified by the breakthrough experiment.⁶

The propagation of magnetoelastic waves is a complex problem which has been intensively studied since 1958.⁹ For many magnetic media the dispersion equation for such waves displays several branches^{10,11} which can be individu-

ally identified with spin waves, magnetostatic waves or elastic waves. Mixed waves coupling magnons and phonons occur principally when branches intersect, so that the frequencies and wavelengths for both are nearly equal.⁸ Away from those values of parameters magnetic and acoustic waves can be separated. This possibility was successfully exploited as a means to propagate only the former to some remote part of a sample where it was desired to magnetically modulate the phases of the states of the nuclei without carrying acoustic noise along to the same place.

The most convenient of the Mössbauer transitions for modulation experiments is the 14.4 keV transition of ⁵⁷Fe diluted in a thin metal foil. The propagation of magnetic waves in conductive foils presents a special problem because of eddy current losses; Kittel has given an approximation⁹ which would limit the mean free path for a magnon to a few wavelengths for the frequencies of tens of MHz which would be interesting for use with ⁵⁷Fe. For this reason the preferred choices for the propagation of magnetization in such thin metallic foils are the magnetostatic waves characterized by long wavelengths and high group velocities^{10,12} that are quite removed from intersections with acoustic branches. Wavelengths can readily reach the scale of millimeters, and it has been demonstrated that dispersion properties are little affected by raising the temperature of the foil above the Curie point.¹³ Thus, if they can be excited at the boundaries, such spin waves should propagate in paramagnetic foils as well as they do in conductive ferromagnetic foils.

Relatively recently, it has been shown¹⁴ how to communicate the large values of magnetization characteristic of ferromagnetic materials into thin foils of paramagnetic media, such as stainless at room temperature, by sandwiching it between ferromagnetic layers. Grünberg demonstrated that at small separations ferromagnetic foils switch coherently so that lines of fringing flux emerging from one continue across to the other. Flux refraction insures that this small normal component is compressed in the separating layer by a factor comparable to its ratio of length to thickness, an aspect ratio of about 10^4 in these experiments. In this way a wave of oscillating magnetization was launched into a stainless tape, enriched in ⁵⁷Fe so that nuclear

phase modulation might be observed at a distance from the source of the disturbance that was greater than the range for the transport of acoustic phonons.⁶

In the absence of these Mössbauer techniques we developed⁶ the detection of spin waves is a very tedious procedure involving neutron scattering resolved with triple spectrometers. Because of this it was decided to try to evaluate the extent to which spin waves could be studied with our more tractable Mössbauer method. The first concern was paid to the attenuation coefficient because that ultimately limits the range over which any other properties can be studied.

Figure 1 shows the experimental arrangement of the propagation medium and spin wave injector. As can be seen the intensity ($\sim H^2$) present in the spin wave at the point of observation is proportional to the relative amplitude of the first order sideband, F_1 it produces on the 14.4 keV line for low levels of excitation and to F_T , otherwise. In particular we measured,

$$F_1 = I_1 \left(\sum_{j=-\infty}^{\infty} I_j \right)^{-1} \quad , \quad (1a)$$

and

$$F_T = \left(\sum_{j=-\infty}^{\infty} I_j \right) - I_0 \quad , \quad (1b)$$

where I_j was the fractional absorption found in the n -th sideband. Figure 2 shows a typical measurement after 2.5 mm of propagation and a standard family of Lorentzian lines fit to the data.

Shown in Fig. 3 is the resulting curve for the attenuation of spin wave intensity at a frequency of 20 MHz in the stainless steel foil 10 mm by 15 mm by $2.5 \mu\text{m}$ in which they were propagated. Each datum represents two separate measurements and the distances along the tape were sampled in no particular order.

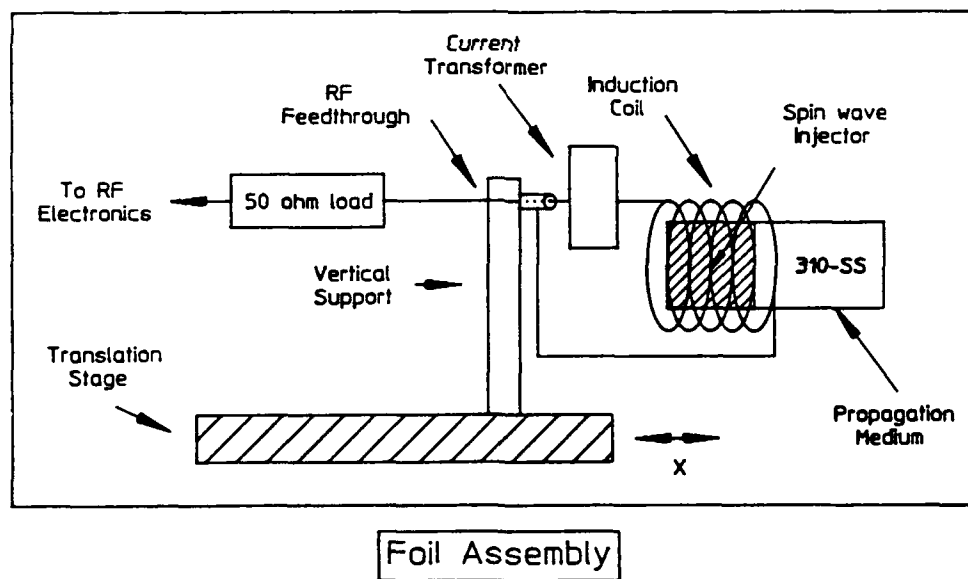
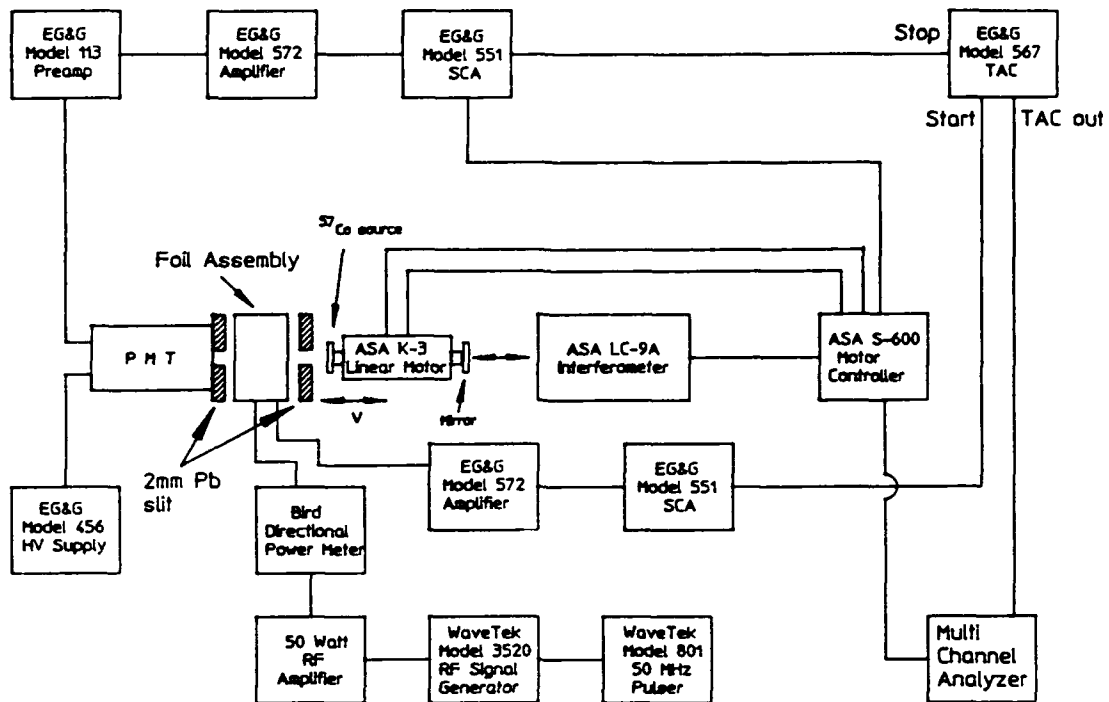


Figure 1: Schematic arrangement used in the studies of spin wave propagation. Details of the mounting of the enriched stainless steel foil serving as a spin waveguide are shown in the inset.

Striking in Fig. 3 is the appearance of what seems to be oscillations around the exponential curve expected to describe the decay. These may be evidence of standing waves and the phasing to show a maximum at the free end of the foil supports this hypothesis. If the distance between nodes represents $\lambda/2$ then the velocity of propagation is

$$v_s = 1 \times 10^7 \text{ cm s}^{-1} \quad , \quad (2)$$

which is much too fast to be acoustic waves. The velocity of sound in this medium should be $v_t = 5.79 \times 10^5 \text{ cm s}^{-1}$ for transverse waves and $v_l = 3.1 \times 10^5 \text{ cm s}^{-1}$ for longitudinal. Spin waves should be faster and in this case they would seem to be. A change of frequencies is needed to confirm this identification.

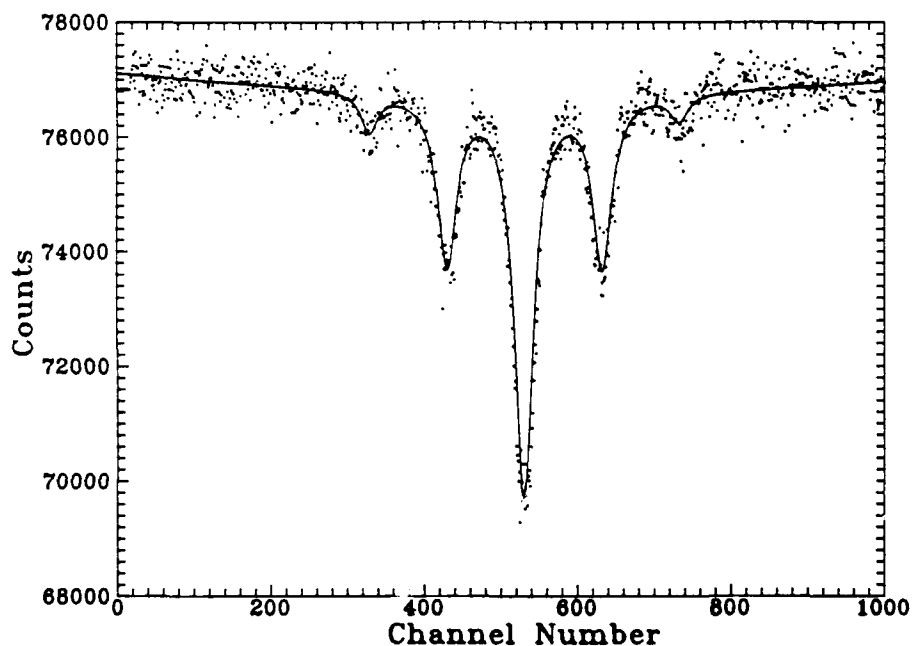


Figure 2: Absorption spectrum of the stainless steel foil with data points showing sidebands excited by spin waves launched at 20 MHz into the foil at a point 2.5 mm from the region of observation. A mathematical fit to the data is shown by the solid curve from which relative intensities were taken.

Before varying frequencies we decided to try to measure the spin wave velocity directly. The same physical arrangement was used but the electronics were changed. As shown in Fig. 1 spin waves were injected into the foil by a ferromagnetic N_i foil in which the magnetization was periodically reversed by the field produced by a radiofrequency (rf) current circulating in a coil containing the foil. In the revised arrangement the rf current was modulated by a square wave. A trigger synchronized with the start of each onset of current was used to start a time to amplitude converter (TAC). The detection of an unabsorbed 14.4 keV photon transmitted through the foil at the point of observation was used to stop the TAC. The resulting output from the TAC was connected to a pulse height analyzer (PHA). After many repetitions the PHA accumulated a histogram showing how many photons had been detected at the point of observation after the various possible delay times following the onset of rf current at the input end of the foil.

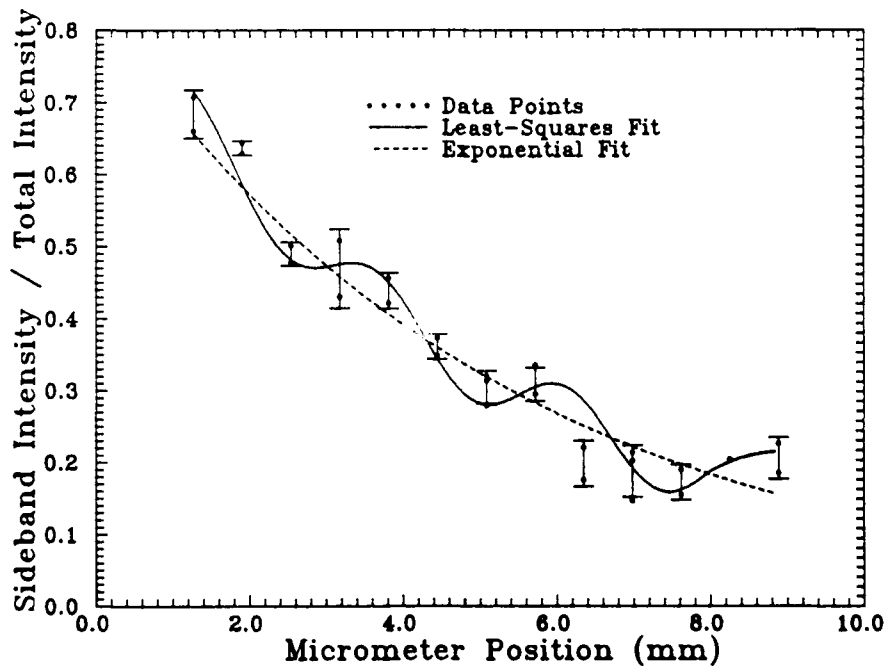


Figure 3: Total relative sideband intensity, F_T measured at 20 MHz as a function of the distance the spin waves traveled from the point of injection to the region of observation.

The ^{57}Co source of probe photons was moved with a constant velocity so that during the period the rf current was flowing, the energy for resonant absorption of 14.4 keV photons was shifted to correspond to that of the first order sideband. For a particular delay time following the onset of the rf current, the likelihood of a γ -photon being transmitted through the foil should have been greater if the spin wave had not yet arrived at the point of observation. This consideration suggested that the PHA output should be a constant counting rate as a function of delay with a downward step signaling the arrival of the spin wave. Figure 4 seems to show such a feature and the delay of 160 ns for this point of observation indicates a lower limit to the velocity, v_s'

$$v_s' \geq 2.0 \times 10^6 \text{ cm s}^{-1} \quad (3)$$

a limit in good agreement with what was indicated by the standing waves in Eq. (2).

To be compelling it is clear the the data of Fig. 4 must be reproduced for different distances of propagation. Then, changes of frequencies should ultimately produce the dispersion curve of velocity as a function of frequency that would carry the unequivocal signature of spin waves. However, this is a very difficult experiment for fundamental reasons. Not more than one photon can be collected for each rf pulse, since the TAC can measure only one interval at a time. Then, to optimize the experiment means to adjust the pulse modulation rate to agree roughly with the counting rate from the Mössbauer source in the spin wave geometry. The result is a very slow experiment. The rate at which a PHA spectrum can be collected is comparable to the frequency of catastrophic failure. The data of Fig. 4 were collected once. A baseline study with the point of observation at the spin wave source showed no step as expected, but those data were destroyed by a power outage associated with the monthly thunderstorm.

While weighing the merits of initiating a dedicated effort to measure the dispersion curve for spin waves against the disadvantages of excluding the equipment from usage in shorter tests of concepts, we were excited by a peculiar new effect which ultimately proved to be of little value. The

primary observation was that if the rf current flowed through the foil in which the observations were made, rather than in a coil around it, sidebands were generated on the 14.4 keV transition. The unusual aspect was that only sidebands of even order appeared.

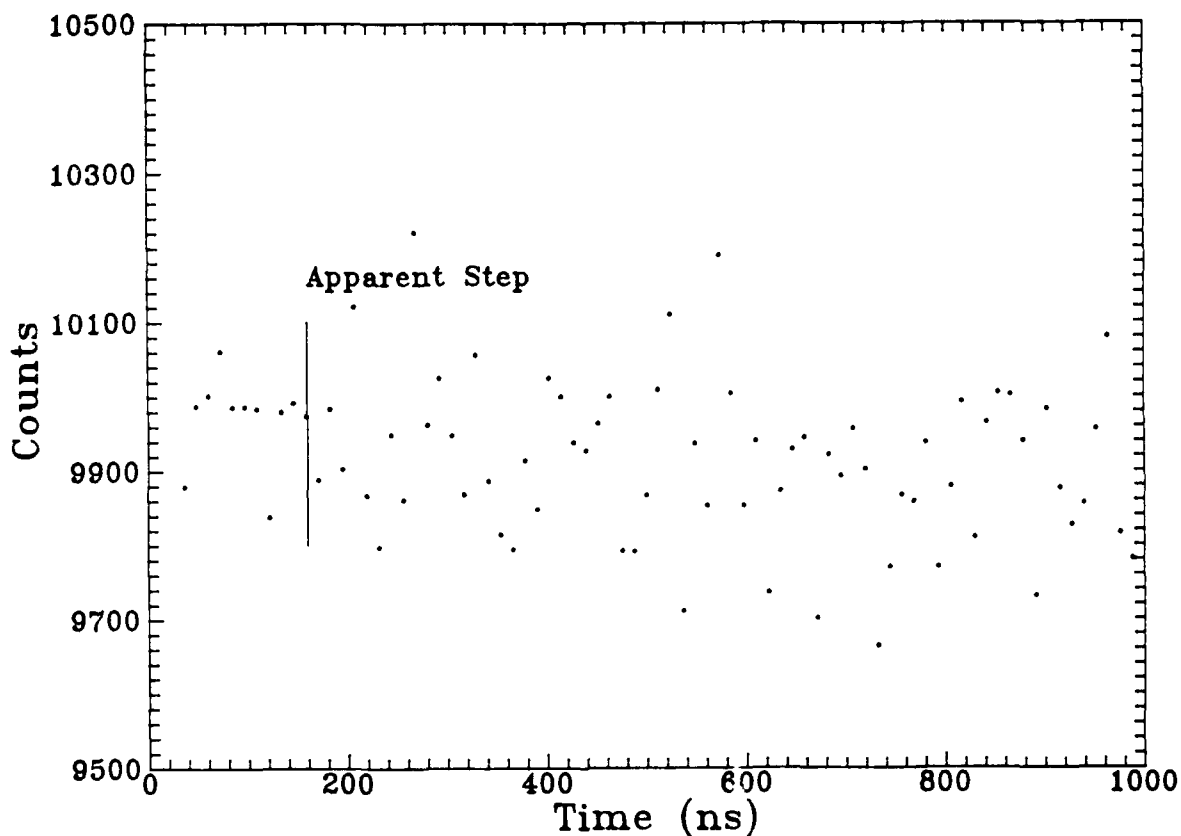


Figure 4: The number of 14.4 keV photons shifted in energy to agree with the peak of one of the first order sidebands in Fig. 2 that passed through the foil without absorption at a point 3.175 mm away from one edge of the source of spin waves propagating in the foil. The abscissa records the times of delay between the injection of a pulse of spin waves of frequency 20 MHz into the foil and the start of a period of 12.2 nsec for recording photons. The arrival of the pulse of spin waves at the point of observation is signaled by the apparent decrease in counting rate caused by the increased absorption as marked.

The arrangement in which current sidebands were excited on the 14.4 keV transition of ^{57}Fe is shown in Fig. 5. Two variants are seen, one passes the current through a stainless steel foil in which observations are made and the other passes the current through a Ni pad pressed onto the stainless foil. There were no coils used. The resulting spectra are seen in Fig. 6. The one excited with the Ni pad shows a normal sideband spectrum with all orders, while the other has only even order sidebands.

Several tests indicated that the sidebands excited with the intermediate Ni foil were simply the spin-wave sidebands resulting from the periodic magnetization of the Ni by the currents flowing through it. The phenomenology in this case was the same as found for the spin wave excitation reported earlier.⁶ In particular, those effects were not sensitive to mounting or to any mechanical damping of spurious vibrations which might have been present in the foil.

Recalling that the spin wave sidebands resulted⁶ from the modulation of the phases $\phi_a(t)$ of the nuclear states involved in the γ transition by the applied magnetic fields, it first seemed that the new sidebands might be the result of a similar modulation of $\phi(t)$ by the currents through the isomer shift.

For cases in which there is no static magnetic field¹⁵ or in which the modulation is parallel to the static field,¹⁶ the effect of the time-varying component $H_0 f(t)$ upon an eigenstate of the nucleus, $\Psi^{(0)}_{a,m}$, can be written

$$\Psi_{a,m} = e^{-i\phi_a(t)} \Psi^{(0)}_{a,m}, \quad (4)$$

where $\phi_a(t)$ is the modulation angle of the phase,

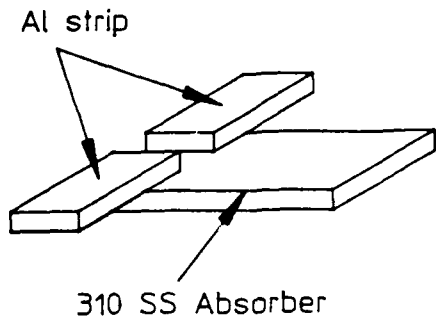
$$\phi_a(t) = m\omega_a \int_0^t f(t') dt', \quad (5)$$

and the Larmor frequency ω_a is

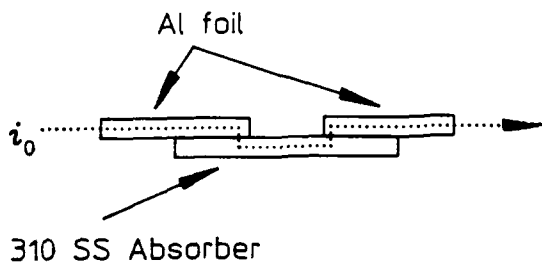
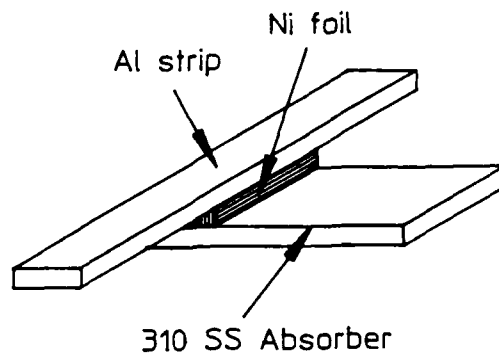
$$\omega_a = \mu_N g_a H_0 / \hbar, \quad (6)$$

where μ_N is the nuclear magneton, g_a is the gyromagnetic ratio for the a th excited or ground state of the nucleus, and m is the magnetic quantum number of the eigenstates.

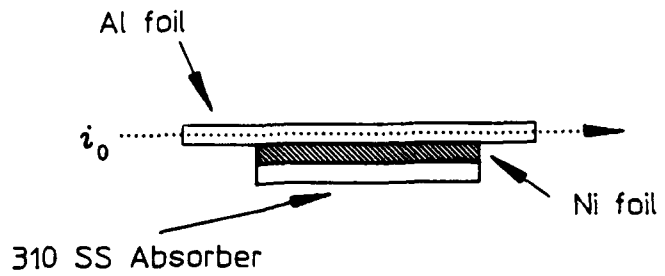
Thermomechanical Sidebands



Spin Wave Sidebands



(a)



(b)

Figure 5: Schematic representation of the arrangement used to excite thermomechanical sidebands (on the left) in comparison to the typical scheme for producing spin wave sidebands (on the right). The path of radiofrequency (rf) current is shown by the dotted arrow.

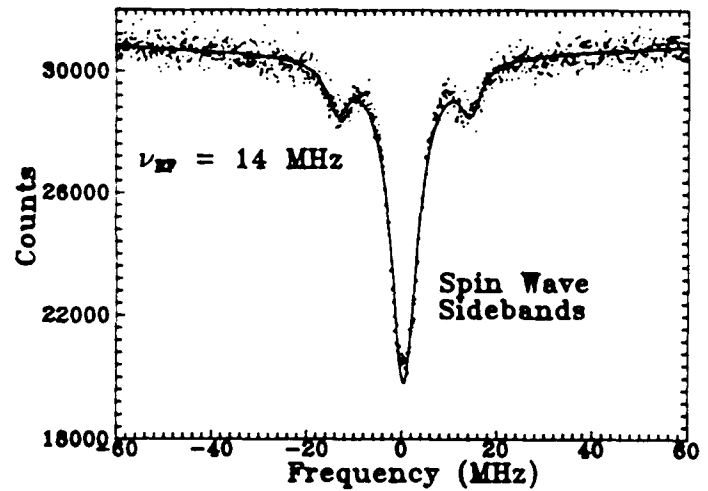
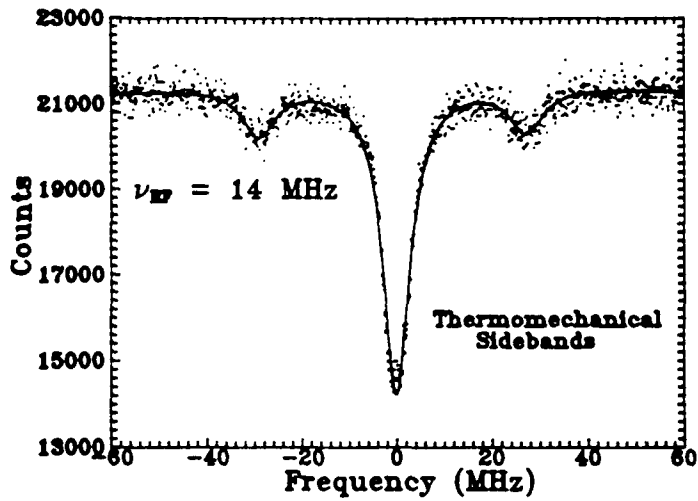


Figure 6: Absorption data obtained with the comparative arrangement of Fig. 5. The spectra were obtained by using constant acceleration between source and absorber to produce a Doppler shift of energies by the amounts shown on the abscissa in frequency units. The positions of the spectra correspond to the arrangements shown in Fig. 5 used to excite them and in both cases the driving frequency was 14 MHz.

It is the difference in phase modulation between the ground state, g , and an excited state, e , that is observed during an absorption transition because the Fourier components of $\phi_e(t) - \phi_g(t)$ are manifested as sidebands.

Inspection of Eq. (4) shows that in the most general sense, nuclear phase can be contributed by any interaction energy between the nucleus and its environment. Our first impression was that the Coulomb interaction between the nucleus and the s -electrons would contribute a phase for which modulation would have the proper symmetry to suppress sidebands of odd order. It is not unusual for conduction electrons in transition metals to include a proportion of those in s -states which mix with the core electron wavefunction. There is a reasonable component of the isomer or chemical shift of nuclear levels from this effect.

Because s -electrons have charge distributions that are spherically symmetric, oscillations back and forth across a nucleus would result in a change of interaction energy that is the same for a perturbation to $+x$ or to $-x$. Then, a mechanism could be conceived in which sinusoidal oscillation of the conduction electrons in the direction of a linear current flow could cause oscillation of the s -electrons in the same direction across the nuclear center resulting in an interaction energy containing a rectified sinusoidal term. That term would give only even orders of sidebands in the Fourier expansion of the resulting nuclear phase. Such an effect would point to a very attractive means of manipulating nuclear states by modulating the isomeric shift, but that did not prove to be the origin of the even sidebands in Fig. 6.

Katila and coworkers¹⁷ have given another nuclear phase associated with the position of the nucleus in a medium as,

$$\phi_x(t) = 2\pi x(t)/\lambda \quad . \quad (7)$$

This, however, is the phase of the origin of the γ -ray emission. From our perspective this is a much less interesting quantity as it does not reflect or affect the internal phase of the nuclear state shown in Eq. (5). The "Katila phase" of Eq. (7) is the one which is produced by vibration or other mechanical effects.

If we assume that the heating associated with the current flowing through a localized portion of the foil causes a linear expansion

$$\Delta x = \alpha \lambda_1 (\Delta T) / 2 \quad , \quad (8)$$

where α is the thermal expansion coefficient and λ_1 is the wavelength for an acoustic vibration with velocity v_1 ; then even order sidebands will be expected. Here, the tacit assumption has been made that only the region within $\lambda_1/2$ around a nucleus can contribute to its displacement by thermal expansion. The effects from regions more remote would tend to excite an acoustic wave that would not be coherent with the one building within the first $\lambda_1/2$ adjacent to the nucleus.

In the arrangement of Fig. 5 the volume, V having resistance R of the foil was heated by the passage of a current,

$$i = i_0 \cos \omega t \quad , \quad (9)$$

and cooled by conduction through the thin dimension into the supporting flat, a microscope cover slide. The time dependence of the temperature rise needed in Eq. (8) is then the solution to the equation,

$$\frac{d(\Delta T)}{dt} = 2Q \cos^2 \omega t - K(\Delta T) \quad , \quad (10a)$$

where,

$$2Q = \frac{i_0^2 R}{C \rho V} \quad , \quad (10b)$$

and $C \rho V$ is the heat capacity of the volume and K is the thermal diffusion coefficient for the sample. Substituting $\cos^2 \omega t = 1/2(1 + \cos 2\omega t)$ gives,

$$\frac{d(\Delta T)}{dt} = Q + Q \cos 2\omega t - K(\Delta T) \quad . \quad (11)$$

For the region heated in Fig. 5, the value of K is important for later simplifying approximations,

$$K = 580 \text{ J/sec/}^\circ\text{C} \quad , \quad (12)$$

and clearly $K \ll \omega$ which was of the order of MHz.

The steady-state solution to Eq. (11) for the condition $K \ll \omega$ is closely approximated by,

$$\Delta T = B + \frac{Q}{2\omega} \sin 2\omega t \quad , \quad (13)$$

where B is the asymptotic temperature rise in the limit of longer times. Substituting Eq. (10b) into (13) and then into Eqs. (8) and (7) gives,

$$\phi_x(t) = \frac{2\pi x_o}{\lambda\gamma} \sin 2\omega t \quad , \quad (14a)$$

where

$$x_o = \frac{\alpha i_o^2 R \lambda_1}{4C\rho V\omega} \quad , \quad (14b)$$

and $\lambda\gamma$ is the wavelength of the 14.4 keV γ photon. In Eq. (14a) the asymptotic phase change associated with the thermal expansion of the foil to the steady state temperature, B in Eq. (13) has been dropped.

In the configuration of Fig. 5 the volume represented a 1 cm² portion of the foil 8 μ m thick with an R ~ 1 Ω . At an rf current of the order of 10 A for a frequency of $2\pi\omega$ ~ 10 MHz the amplitude of the phase change in Eq. (14a) is

$$\phi_o = \frac{2\pi x_o}{\lambda\gamma} = 0.1 \quad . \quad (15)$$

The quantity of Eq. (15) is equivalent to the modulation index of a carrier wave and is a measure of the amount of spectral intensity appearing in the lowest order sideband. This can be appreciated by considering that the nucleus emits a γ wave in the x-direction described by,

$$\bar{E} = \bar{E}_o e^{i(kx - \omega_\gamma t + \phi_x(t))} \quad . \quad (16)$$

Substituting Eq. (14a) into (16) gives

$$\bar{E} = \bar{E}_o e^{i(kx - \omega_\gamma t + \phi_o \sin 2\omega t)} \quad . \quad (17)$$

For this problem a useful phasing of the Jacobi-Anger expansion is

$$e^{iz \sin 2\omega t} = \sum_{m=-\infty}^{\infty} J_m(z) e^{i2m\omega t} \quad . \quad (18)$$

substituting this into Eq. (17) gives for the propagating γ wave,

$$\bar{E} = \bar{E}_o e^{i(kx - \omega_\gamma t)} \sum_{m=-\infty}^{\infty} J_m(\phi_o) e^{i2m\omega t} \quad , \quad (19a)$$

$$- \bar{E}_0 e^{i(kx - \omega_\gamma t)} \sum_{m=-\infty}^{\infty} J_m(\phi_0) e^{i2m\omega t} \quad , \quad (19b)$$

$$- \sum_{m=-\infty}^{\infty} \bar{E}_0 J_m(\phi_0) e^{i(kx - [\omega_\gamma - 2m\omega]t)} \quad . \quad (19c)$$

The interpretation of Eq. (19c) is that the γ -ray is a sum of components with frequencies $(\omega_\gamma \pm 2m\omega)$ and relative amplitudes of $J_m(\phi_0)$. Since intensity is basically E^2 the relative intensity, I_m of the m -th sideband is

$$I_m = I_0 J_m^2(\phi_0) \quad , \quad (20)$$

again where ϕ_0 is the modulation index.

While $f_0 \sim 0.1$ is too small to explain the size of the sidebands seen in Fig. 6, it is suggestively close. One half order of magnitude increase would explain them and this is about as close as theory and experiment have agreed in the experiments of others designed to produce acoustic sidebands. The important feature is that Eq. (19) predicts only even order sidebands and that is what is seen in Fig. 6. The data shown there represent the first time such sidebands have been seen in Mössbauer spectroscopy without any odd orders appearing.

The rough agreement between theory and experiment strongly suggests that the new type of sidebands seen in Fig. 6 have a thermomechanical origin. The likelihood that such a curious phenomena has this trivial origin is supported by the observations that it is very easy to damp them mechanically. Unlike the spin wave sidebands, the phenomenon of Fig. 6 can be eliminated by contacting the foil to some soft material. In the absence of any indications that there was an unquenched component which might have arisen from a modulated isomer shift, this effect was not investigated further.

Along the second effort pursued during the past year, instrumentation was developed to study tagged photons. The intent is to select γ photons for those associated with unusually long wavetrains so that higher spectroscopic resolution may be achieved. With the ^{57}Fe system this can be done because the 3/2- state radiating the 14.4 keV Mössbauer line is populated by cascade from a 5/2- state lying at 136.5 keV. Emission of the 5/2- to 3/2- photon at 122

keV provides a timing mark at the instant the $3/2^-$ state is created. The selection can then be made to accept 14.4 keV photons only after a certain time has elapsed after receipt of a timing mark.

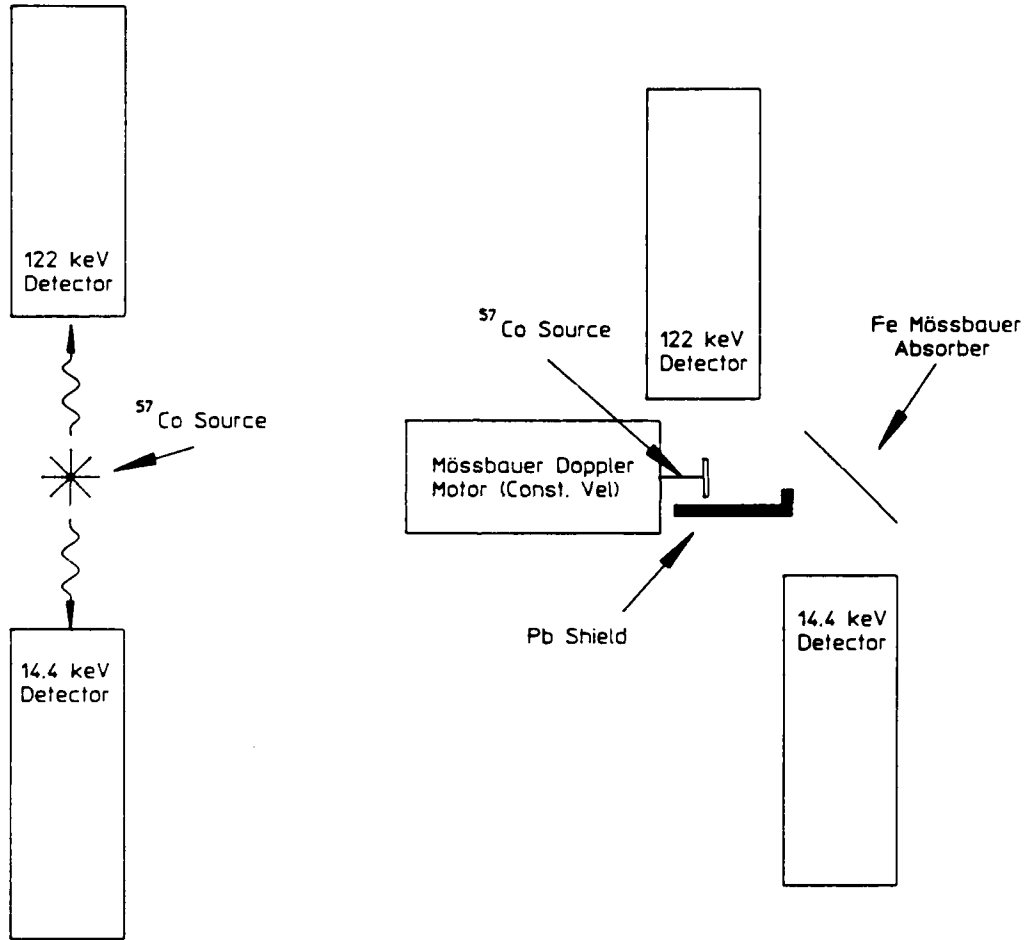


Figure 7: Schematic representation of the two arrangements used to demonstrate tagged photon capabilities.

The concept is not new and the power of the technique was demonstrated by Hoy¹⁸ in 1968 in a beautiful series of experiments demonstrating the variability of the spectroscopic resolution that could be achieved. However, in his work the data collection was limited to such low rates that weeks were required for a spectrum. Our first intent was to exploit the advances in electronics that accommodate much higher discrimination rates than were possible in 1968. Then it was planned to use the selected wavetrains to look for the nodes and antinodes in absorption and emission that Harris predicts. In that application we need to select for accidentally shortened wavetrains so the natural line widths will occupy a more favorable fraction of the spacing between lines.⁵

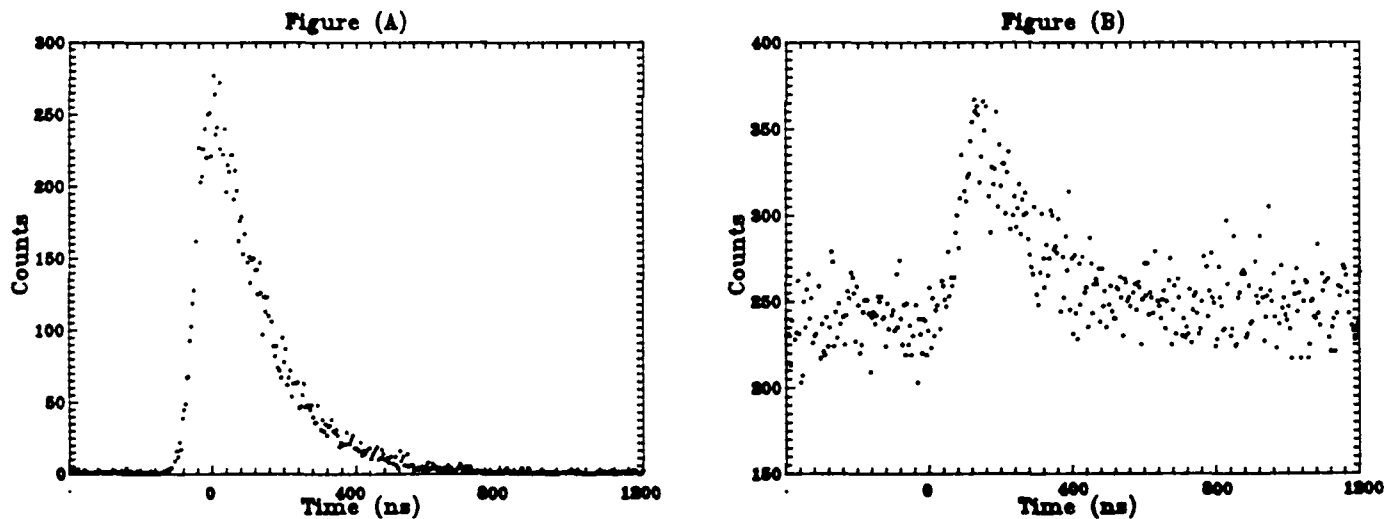


Figure 8: Counting rates for the detection of 14.4 keV photons as function of the time elapsed between preparation of the radiating state and emission of a photon from it for the two arrangements shown in Fig. 7.

During the present reporting period we concentrated on the two arrangements shown in Fig. 7. The one involving only the source served for calibration and the data shown in the left panel of Fig. 8 illustrates the capabilities for rapid data collection. It was obtained in 10 min. of experimental time.

The arrangement seen in the right panel of Fig. 7 is the more appropriate with which to look for interference structure. Without consideration of any changes in the bandwidths caused by resonant absorption and reemission, the fluorescence intensity from a target illuminated as shown to the right of Figure 7 should be

$$I \sim I_0(t/\tau)e^{-t/\tau} \quad , \quad (21)$$

where τ is the natural lifetime of the $3/2^-$ state. It can be readily seen that the data to the right of Fig. 8 is quite different from that to the left in that it follows the general form of Eq. (21).

The next step along this line is to utilize the option to tune the relative velocity of source and fluorescence target to excite just one m_j component of the $3/2^-$ state and then to begin to look for the predicted interferences. In that experiment instead of the 14.4 keV fluorescence the 6 keV x-ray will be detected. The m_j levels of the $3/2^-$ state lie in the continuum for internal conversion and that process is blind to the origin of the $3/2^-$ population. This seems to be just the nuclear analogy of Harris' ideal atomic states having natural width and lying within the continuum for autoionization. At our nuclear level the internal conversion of the state is first being detected by the K_α x-ray from the iron that results from an electron filling the $1s$ vacancy created by the internal conversion event. Under final testing is a second system using a microchannel plate (MCP) for the direct detection of the electron emitted during the creation of the $1s$ hole. That effort lies at the focus of the third line pursued under this grant during the past year.

Figure 9 shows a schematic representation of the apparatus for tagged photons constructed along the third line of effort devoted to improved instrumentation. In continuing the comparison between double resonance

experiments at the atomic scale and (γ, γ') reactions at the nuclear level, the principal differences should be noted because they dominate the design of apparatus such as shown in Fig. 9

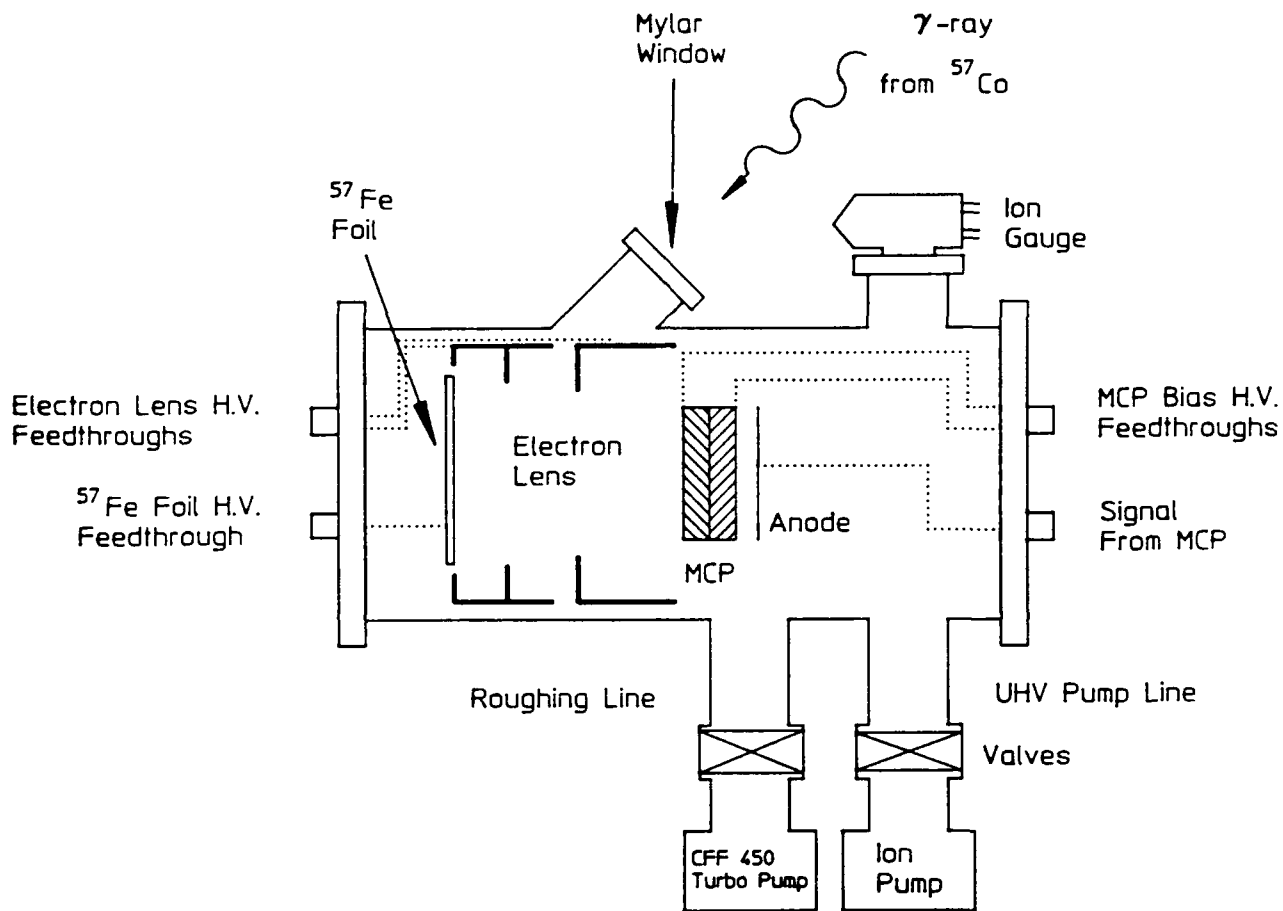


Figure 9: Vacuum system and apparatus to support the detection of tagged photon events by the internal conversion electrons emitted.

In the atomic domain of energies, the experimental apparatus is generally "black" unless explicit efforts are made to render it reflective. Just the opposite is the case at the nuclear level. For most materials the efficiency

for x-ray fluorescence from the atomic electrons in the bulk exceeds 50% so graded absorbers from sequences of successively lighter materials are required. If any sources of higher energy photons are present, Compton scattering can shift them down into the region of Mössbauer energies. Simply assembling an apparatus according to standards appropriate for atomic experiments would result in a very "bright" environment in which nuclear signal events would be submerged in the noise from atomic x-rays. Considerable care has been taken in the design and construction of the apparatus of Fig. 9. In Fig. 10 is an example showing the design of electrostatic elements to steer and focus the conversion electrons from a fluorescence target to an MCP placed to be unable to see any direct sources. Of course, all vacuum must be maintained without vibrating any of the nuclear samples to preserve the Mössbauer spectra. In operation only the ion pump is used while being heavily screened to avoid the escape from it of either particles or soft x-rays.

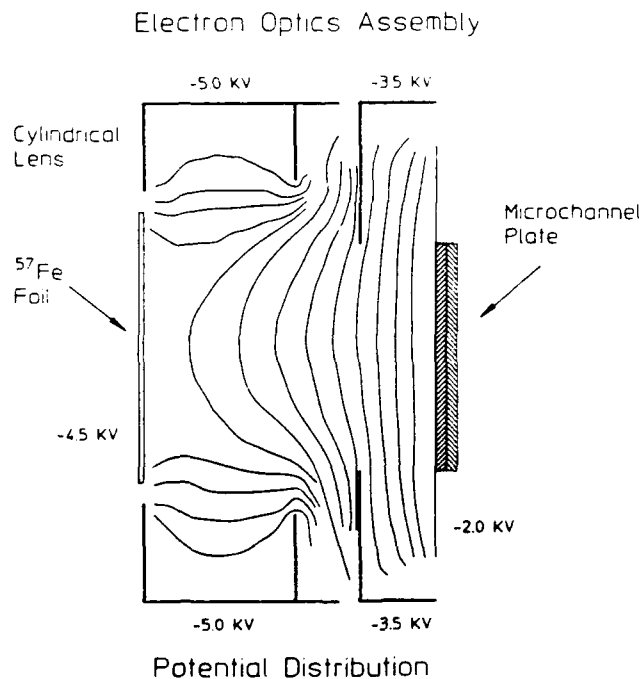


Figure 10: Calculated electric field patterns used to draw electrons from the target for nuclear fluorescence to the MCP for detection.

Figure 11 shows a Mössbauer spectrum obtained by collecting the conversion electrons from the ferromagnetic ^{57}Fe target shown in Fig. 9 when illuminated by an unsplit source moved with constant acceleration. At the time of reporting the first experiments are being done to tag the photons giving the spectrum of Fig. 11.

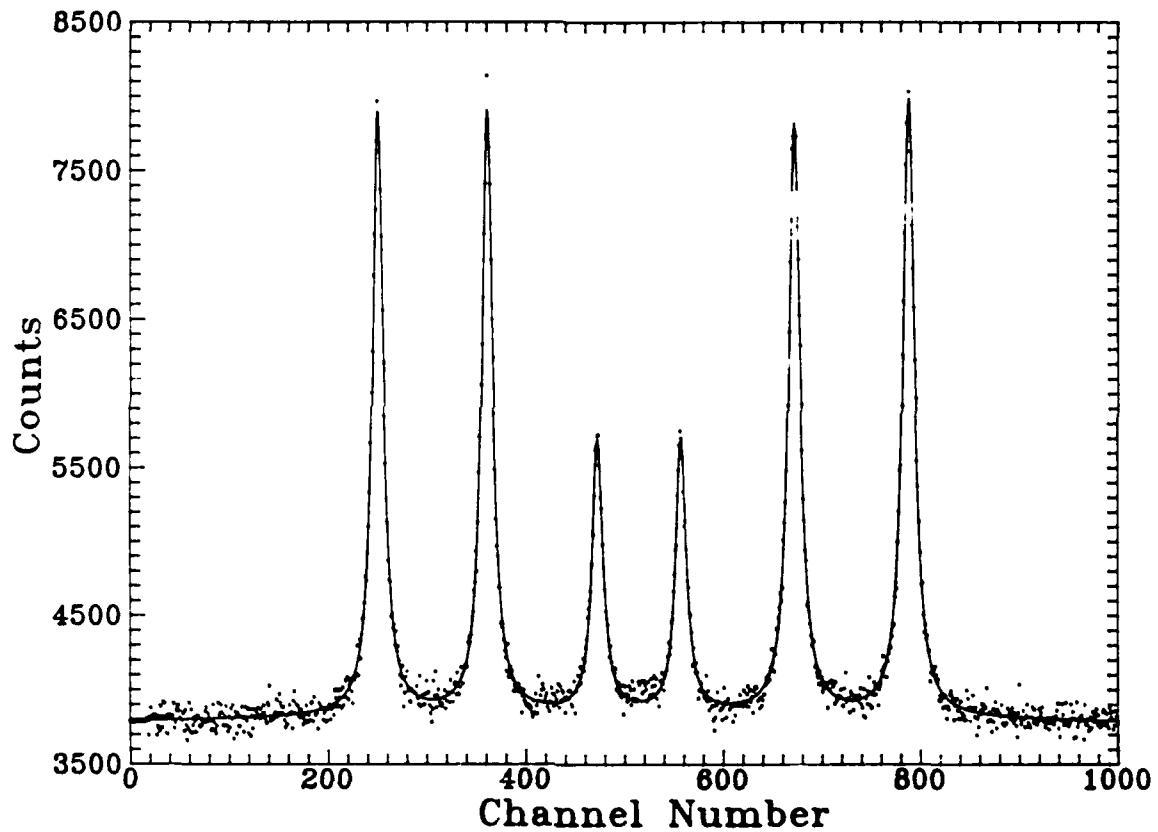


Figure 11: Mössbauer fluorescence spectrum obtained with the apparatus of Fig. 9 without yet using the photon tagging capability.

While this current reporting period is not completed at the time of writing, it can be expected that the remainder of the period will see continued linear progress from this point.

REFERENCES

1. C. B. Collins, J. A. Anderson, F. Davanloo, C. D. Eberhard, J. J. Carroll, J. J. Coogan, and M. J. Byrd, *Lasers and Part. Beams* 7, 357 (1989).
2. C. B. Collins, C. D. Eberhard, J. W. Glesener, and J. A. Anderson, *Phys. Rev. C* 37, 2267 (1988).
3. C. B. Collins, J. J. Carroll, T. W. Sinor, M. J. Byrd, D. G. Richmond, K. N. Taylor, M. Huber, N. Huxel, P. v. Neumann-Cosel, A. Richter, C. Spieler, and W. Ziegler, *Phys. Rev. C.* (accepted).
4. C. B. Collins, F. W. Lee, D. M. Shemwell, B. D. DePaola, S. Olariu, and I. I. Popescu, *J. Appl. Phys.* 53, 4645 (1982).
5. S. E. Harris, *Phys. Rev. Lett.* 62, 1033 (1989).
6. T. W. Sinor, P. W. Reittinger, and C. B. Collins, *Phys. Rev. Lett.* 62, 2547 (1989).
7. C. B. Collins, F. Davanloo, E. M. Juengerman, W. R. Osborn, and D. R. Jander, *Appl. Phys. Lett.* 54, 216 (1989).
8. F. Davanloo, E. M. Juengerman, D. R. Jander, T. J. Lee, and C. B. Collins, *J. Appl. Phys.* 67, 2081 (1990).
9. C. Kittel, *Phys. Rev.* 110, 836 (1958).
10. P. C. Fletcher and C. Kittel, *Phys. Rev.* 120, 2004 (1960).
11. E. Schlömann, *J. Appl. Phys.* 31, 1647 (1960).
12. R. W. Damon and J. R. Eshback, *J. Appl. Phys. Suppl.* 31, 1045 (1960).
13. H. A. Mook, J. W. Lynn, and R. M. Nicklow, *Phys. Rev. Lett.* 30, 556 (1973).
14. P. Grünberg, *J. Appl. Phys.* 51, 4338 (1980).
15. P. J. West and E. Matthias, *Z. Phys. A* 228, 369 (1978).
16. S. Olariu, I. Popescu, and C. B. Collins, *Phys. Rev. C* 23, 1007 (1981).
17. P. Helisto, E. Ikonen, T. Katila, and K. Riski, *Phys. Rev. Lett.* 49, 1209 (1982).
18. D. W. Hamill and G. R. Hoy, *Phys. Rev. Lett.* 21, 724 (1968).

APPENDIX I

Reprint of work published during this reporting period.

"Mössbauer Isomer Shift Measurements without Mechanical Tuning,"
T. W. Sinor, P. W. Reittinger, and C. B. Collins, Rev. Sci. Instrum 60, 3258
(1989).

Mössbauer isomer shift measurements without mechanical tuning

T. W. Sinor, P. W. Reittinger, and C. B. Collins

Center for Quantum Electronics, University of Texas at Dallas, P. O. Box 830688, Richardson, Texas 75083-0688

(Received 16 March 1989; accepted for publication 28 June 1989)

A technique is described which demonstrates how a frequency modulation spectrometer (FMS) can be used to measure the isomer shift of ferromagnetic absorbers without mechanical tuning. As an example, the isomer shift of an iron sample relative to a ^{57}Co source in a Pd matrix was measured and found to be $-(0.1869 \pm 0.003)$ mm/s compared to the literature value of $-(0.185 \pm 0.02)$ mm/s.

INTRODUCTION

The high Q of a Mössbauer resonance, approximately 10^{12} for ^{57}Fe , provides photons of well-defined energy in the keV range that are useful for probing phenomena involving very small changes of energies. In this way Mössbauer spectroscopy can provide a highly detailed account of the way in which the nucleus interacts with its environment. It is only through the existence of the Mössbauer effect that a practical source of narrow line radiation can be produced at these wavelengths, and with such a source very small changes in frequency can be measured.

With Mössbauer techniques there is sufficient frequency resolution that spectral changes produced by magnetic perturbations to the nucleus can be observed in the short wavelength limit where quantum effects are dominant. In particular the Mössbauer effect is ideally suited to the study of the interaction of the nucleus with a rapidly oscillating magnetic field. Mitin^{1,2} was the first to propose that Mössbauer transitions could be excited as part of a multiphoton interaction for nuclei immersed in intense radio-frequency fields. The earliest experiments investigating the influence of radio-frequency magnetic fields on Mössbauer transitions was reported by Perlow³ in 1968. In his experiment, Perlow subjected several ^{57}Co sources of the 14.4-keV transition of ^{57}Fe to intense magnetic fields oscillating at rf frequencies and was able to demonstrate the destruction of the Mössbauer hyperfine pattern by the action of the rf field. Later researchers⁴ soon found that when a ferromagnetic iron absorber was subjected to long wavelength photons of an alternating magnetic field with frequency Ω (MHz), the Mössbauer spectrum contained additional absorption lines, known as rf sidebands, at frequencies $\omega, \pm n\Omega$ where ω is the frequency of the parent transition and $n = 1, 2, \dots$, but these were shown to be artifacts produced by spurious acoustic noise generated in the absorber. True sum and difference frequency lines were not found in Mössbauer spectra until much later.⁵⁻¹⁰ The origin of these tunable sidebands in multiphoton or nuclear phase modulation effects was established even more recently.¹¹⁻¹⁴

The frequency dependence of these rf sidebands provides the basis for development of a high resolution gamma-ray spectrometer which operates by modulating the cross section for the gamma-ray absorption. A prototype of this Frequency Modulation Spectrometer (FMS) was first de-

scribed¹⁰ by our laboratory in 1985 with subsequent refinements¹⁵ reported in 1988.

A FMS spectrum of ^{57}Fe provides a direct measurement of rf sideband positions and intensities without interference from the parent transitions. It does this by scanning the frequency of the probing sidebands¹⁵ as opposed to the shifting of the transition energy conventionally employed. In such a spectrum one can extrapolate information about the transitions between Zeeman split energy levels (parent transitions) and the nuclear isomer shift between the source and absorber. In particular, it provides a technique for accurately measuring the isomer shift directly in terms of frequency; a quantity which can be measured more precisely than the customary Doppler velocity.

The heart of the Frequency Modulation Spectrometer is an Apple II+ computer which serves as a Multichannel Scaler (MCS) and an IEEE-488 GPIB interface as shown in Fig. 1. The GPIB enables the spectrometer to sweep continuously through the frequencies of the rf magnetic field which is controlled by a Wavetek frequency synthesizer. A Mössbauer linear motor allows the frequency of the incident gamma rays to be biased by a constant Doppler shift, if desired. The spectrometer currently has an instrumental resolution of 100 Hz and a frequency range of 1 MHz–1 GHz with a stability of 0.1 Hz/s when used with a stationary source.

In Fig. 2(a) a conventional Mössbauer spectrum of ^{57}Fe showing the six allowed magnetic transitions is shown without external perturbation. Component lines are labeled 1 through 6 with the transition of lowest energy identified as number 1. In the spectrum of the same absorber subject to the excitation of rf sidebands as shown in Fig. 2(b), the sidebands have been labeled using the following nomenclature. The first digit corresponds to the order of the sideband n , with the second number corresponding to its particular parent transition, p . The sign of n indicates whether the sideband appears at a higher ($+n$) or lower ($-n$) energy than its parent transition. For example, $-1;5$ denotes the first order sideband displaced to lower energies from parent transition 5.

The parent transitions 1 and 6 of Fig. 2(a) are symmetric about the centroid of the resonance pattern and are separated by 123.68 MHz. The application of a 61.84 MHz alternating magnetic field to the ^{57}Fe absorber produces $+1;1$ and $-1;6$ sidebands which overlap at the center of the hyperfine structure of the Mössbauer spectrum. The energies of

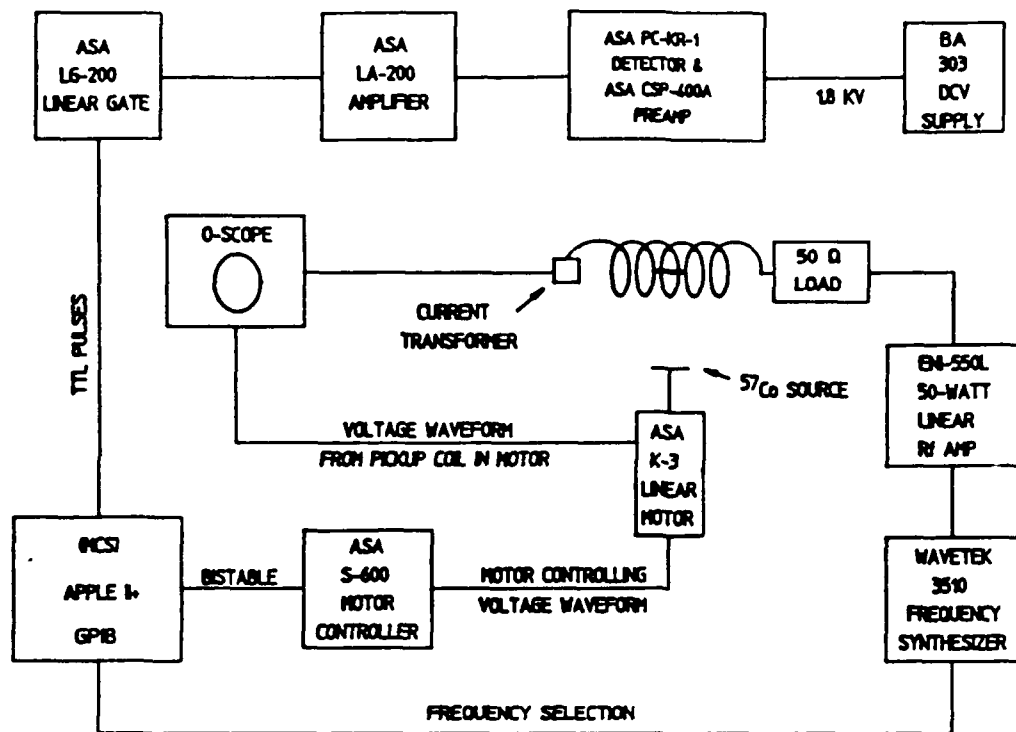


FIG. 1. Schematic representation of a frequency modulation spectrometer (FMS).

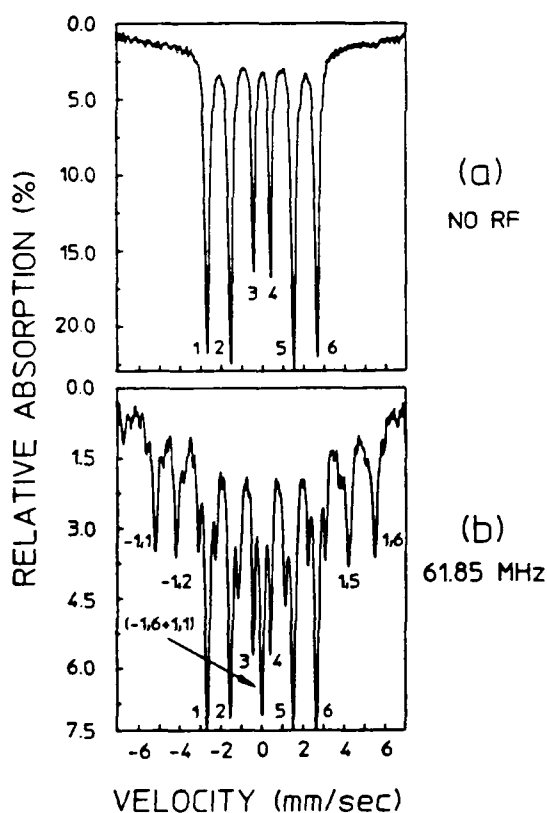


FIG. 2. (a) Mössbauer absorption spectrum of a 2.5- μm foil of iron isotopically enriched with 95.8% ^{57}Fe obtained with a ^{57}Co source in a Pd matrix. The six allowed magnetic dipole transitions are labeled 1 through 6 going from the lowest- to the highest-energy transition. (b) Spectrum of the same foil subjected to an oscillating radio-frequency field with a frequency of 61.85 MHz.

the incident gamma rays from the source will differ from the transition center of the absorber by the isomer shift, Δ . In a FMS spectrum the sidebands $+1;1$ would be observed at a frequency of $(61.85 - \Delta)$ MHz while the sideband $-1;6$, would be detected at a frequency of $(61.85 + \Delta)$ MHz. Therefore, the FMS spectrum will produce two absorption peaks as shown in Fig. 3(a), around 62 MHz with a separation equal to twice the isomer shift, 2Δ . If the Mössbauer source is given a constant velocity Doppler shift, the FMS spectrum will show two peaks near 62 MHz, separated by $2(\Delta + \delta)$, where δ is the Doppler shift of the incident gamma rays. In this way very precise measurements of the nuclear isomer shift can be obtained using FMS. The accuracy of the measurement is dependent upon the resolution and stability of the signal generator used to produce the rf magnetic field and the quality of the curve fitting routine used to fit the data.

I. THEORY

In a Mössbauer absorption spectrum taken in the velocity domain the isomer shift appears as a displacement of the centroid of the resonance pattern from the nominal zero position. The isomer shift is the result of an electric monopole interaction between the Mössbauer nuclei and its surrounding electrons. More specifically, the excited and ground-state nuclei differ in radius by a small yet significant amount ($\Delta R/R = -0.8 \times 10^{-3}$ in ^{57}Fe). It is this change in the radius of the nucleus which causes the electrostatic interaction between the nucleus and its surrounding electrons to change upon excitation of the nucleus. Therefore, if the Mössbauer nuclei in the source and absorber are in different

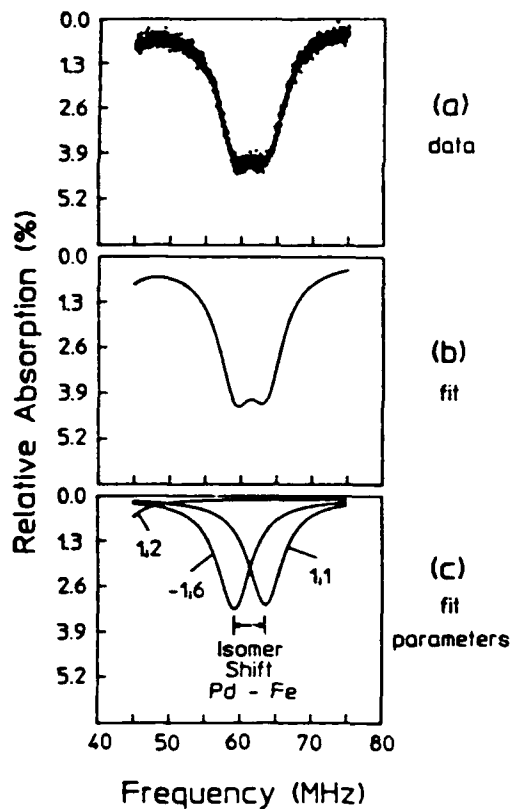


FIG. 3. (a) FMS spectrum of the same enriched foil. The two peaks represent sidebands +1;1 and -1;6. The separation of these peaks is equal to twice the isomer shift of an iron foil relative to a ^{57}Co source in Pd. (b) Spectrum constructed from fitting the data of Fig. (a) using the Levenberg-Marquardt method for a nonlinear least-squares fit. (c) Spectral components resulting from the fitting procedure shown before summation.

chemical environments such that different electronic distributions are experienced, the isomer shift has been shown to be¹⁶

$$\Delta = (4\pi c Z e^2 R^2 / 5 E_\gamma) [\rho_o(0) - \rho_s(0)] (\Delta R / R) \text{ mm/s}, \quad (1)$$

where Z is the atomic number, e is the electronic charge, R is the effective nuclear radius, c is the velocity of light, $\rho_o(0)$ and $\rho_s(0)$ are the electronic charge densities at the nucleus for the source and absorber, and $\Delta R = R_{\text{excited}} - R_{\text{ground}}$.

In addition to the isomer shift displacement of the centroid of the resonance pattern there is also a temperature shift of the spectrum which arises due to time dilation resulting from the motions of the emitting and absorbing nuclei. This temperature shift is given by¹⁷

$$\delta E / E = C_p / 2c^2 \quad (2)$$

where C_p is the specific heat of the material and c is the velocity of light. At room temperature, for iron the above expression yields $\delta E / E = -2.21 \times 10^{-15} / ^\circ\text{C}$. The experimentally observed value¹⁸ is $-(2.09 \pm 0.24) \times 10^{-15} / ^\circ\text{C}$. In the work being reported here the source and absorber were at essentially the same temperature. Therefore, the temperature shift was considered negligible.

The frequency, f_n , at which sidebands appear in a FMS spectrum is given by

$$f_n = (v - P_i + \Delta)(K/n), \quad (3)$$

where v (mm/s) is the Doppler velocity of the source, P_i (mm/s) is the position of the i th parent transition, Δ (mm/s) is the isomer shift, $K (= 11.605 \text{ MHz/mm/s})$ is the conversion factor for the 14.4-keV gamma rays being detected and n is the order of the sideband of interest. Furthermore, it is known that the frequency displacement Ω of sidebands 1;1 and -1;6 is given by

$$\Omega(1;1) = \Omega(-1;6), \quad (4)$$

with respect to the center of the resonance pattern. Therefore, for a stationary source and absorber we have

$$\begin{aligned} \Omega(1;6) - \Omega(1;1) &= |\Omega(P_o) + \Delta| \\ &- |\Omega(P_i) + \Delta| = 2\Delta. \end{aligned} \quad (5)$$

The absolute value of the Ω 's are used since Eq. (3) can result in a negative frequency. However, the sign of f_n is merely a convention to indicate whether the sideband has a lesser or greater energy than its parent transition. The sign convention used for isomer shift measurements is that a negative isomer shift indicates the source has a higher nuclear energy level than the absorber.

II. DATA AND DISCUSSION

The isomer shift between a ^{57}Co source in a Pd matrix relative to an iron foil absorber was measured using FMS and found to have a value of $-(0.1869 \pm 0.003) \text{ mm/s}$ compared to the literature value¹⁹ of $-(0.185 \pm 0.02) \text{ mm/s}$. The ^{57}Co source in a Pd matrix had an initial activity of 25.4 mCi and was purchased from New England Nuclear. The absorber was a $1.5 \text{ cm} \times 0.85 \text{ cm} \times 2.5 \mu\text{m}$ foil of iron isotopically enriched with 95.8% ^{57}Fe . The rf signal was produced by a Wavetek signal generator, Model 3520, which was equipped with an IEEE-488 GPIB interface to allow the frequency to be automatically scanned. The resolution and stability of this signal generator are those previously stated. The rf signal from the Wavetek was amplified by an ENI-5506 50db linear amplifier and this amplified signal was then used to drive an inductor in which the absorber was mounted. A five-turn flat coil was constructed as the field induction coil with a separation of 4.5 mm between turns and a cross-sectional area of 20 mm^2 . This led to a small inductance ($< 1 \mu\text{H}$) and a minimum capacitance between turns while producing a reasonable field intensity ($\sim 4\text{G}$) at 50 W. This inductor was then mounted in series with a 48- Ω noninductive load to match the impedance of the amplifier output and cable. The result was a circuit having a reasonably broad band tunability and a Q of approximately one. The heat produced in the absorber by eddy currents was minimal for the rf powers employed. However, in critical measurements of the isomer shift using FMS, this minimal rf heating of the absorber can be eliminated by simultaneously pulsing the rf and directing a cool flow of nitrogen over the absorber.

The data from which the fitted parameters were obtained is shown in Fig. 3(a). The data was fit to seven parameters using the Levenberg-Marquardt method²⁰ for a nonlinear least squares fit. In the fitting procedure, it was assumed that the spectra were composed of three sidebands; the -1;6, +1;1, and -1;5. It was further assumed that

the sidebands had a uniform linewidth. Figure 3(b) shows the spectrum constructed from the fit parameters and Fig. 3(c) shows the spectral components before summation. The standard deviation of the fit parameters was obtained from the covariance matrix derived from the fitting procedure and are valid only with the assumption of normally distributed measurement error.

As can be seen from this example, FMS is a high-resolution Mössbauer technique which provides a direct measurement of rf sideband positions and intensities without interference from the parent transitions. Furthermore, from an FMS spectrum, information can be obtained without mechanical tuning about the linewidth or positions of Zeeman split energy levels in addition to accurate measurement of the nuclear isomer shift. Recently¹⁴ it has been demonstrated how to excite large-scale magnetic phase modulation effects in paramagnetic materials by exciting magnetostatic spin waves in the sample under study. With this refinement frequency modulation spectroscopy can now be extended to the study of paramagnetic materials. Then, FMS can provide a viable alternative for precision isomer shift measurements in a variety of environments.

ACKNOWLEDGMENTS

The authors acknowledge the support of this work by the Office of Naval Research and by the Innovative Science and Technology Directorate of the Strategic Defense Initia-

tive Organization with direction by the Naval Research Laboratory.

- ¹A. V. Mitin, Zh. Eksp. Teor. Fiz. **52**, 1596 (1967) [Sov. Phys. JETP **25**, 1062 (1967)].
- ²A. V. Mitin, Dok. Akad. Nauk SSSR **194**, 59 (1971) [Sov. Phys. Dokl. **15**, 827 (1971)].
- ³G. J. Perlow, Phys. Rev. **172**, 319 (1968).
- ⁴N. D. Heiman, L. Pfeiffer, and J. C. Walker, Phys. Rev. Lett. **21**, 93 (1968).
- ⁵P. J. West and E. Matthias, Z. Phys. A **288**, 369 (1978).
- ⁶O. Olariu, I. Popescu, and C. B. Collins, Phys. Rev. C **23**, 50 (1981).
- ⁷O. Olariu, I. Popescu, and C. B. Collins, Phys. Rev. C **23**, 1007 (1981).
- ⁸B. D. DePaola and C. B. Collins, J. Opt. Soc. Am. B **1**, 812 (1984).
- ⁹C. B. Collins and B. D. DePaola, Opt. Lett. **10**, 25 (1985).
- ¹⁰B. D. DePaola, S. S. Wagal, and C. B. Collins, J. Opt. Soc. Am. B **2**, 541 (1985).
- ¹¹T. W. Sinor, Ph.D. thesis, University of Texas at Dallas, 1988.
- ¹²E. Ikonen, P. Helistö, J. Hietaniemi, and T. Katila, Phys. Rev. Lett. **60**, 643 (1988).
- ¹³E. Ikonen, J. Hietaniemi, and T. Katila, Phys. Rev. B **38**, 6380 (1988).
- ¹⁴T. W. Sinor, P. W. Reittinger, and C. B. Collins, Phys. Rev. Lett. **62**, 2547 (1989).
- ¹⁵P. W. Reittinger, T. W. Sinor, S. S. Wagal, and C. B. Collins, Rev. Sci. Instrum. **59**, 362 (1988).
- ¹⁶See, for example, G. K. Shenoy and F. E. Wagner, Eds. *Mössbauer Isomer Shifts* (North-Holland, Amsterdam, 1978).
- ¹⁷B. D. Josephson, Phys. Rev. Lett. **4**, 341 (1960).
- ¹⁸R. V. Pound and G. A. Rebka, Jr., Phys. Rev. Lett. **4**, 274 (1960).
- ¹⁹A. H. Muir, Jr., K. J. Ando, and H. M. Coogan, *Mössbauer Effect Data Index, 1958-1965* (Wiley-Interscience, New York, 1966).
- ²⁰B. P. Flannery, S. A. Teukolsky, and W. T. Vetterling, *Numerical Recipes: The Art of Scientific Computing* (Cambridge University Press, Cambridge, 1985).